

# Relativistic stellar aberration for the Space Interferometry Mission

Slava G. Turyshev<sup>1</sup>

*Jet Propulsion Laboratory, California Institute of Technology, Pasadena, CA 91109*

## ABSTRACT

This paper analyses the relativistic stellar aberration requirements for the Space Interferometry Mission (SIM). We address the issue of general relativistic deflection of light by the massive self-gravitating bodies. Specifically, we present estimates for corresponding deflection angles due to the monopole components of the gravitational fields of a large number of celestial bodies in the solar system. We study the possibility of deriving an additional navigational constraints from the need to correct for the gravitational bending of light that is traversing the solar system. It turns out that positions of the outer planets presently may not have a sufficient accuracy for the precision astrometry. However, SIM may significantly improve those simply as a by-product of its astrometric program. We also consider influence of the higher gravitational multipoles, notably the quadrupole and the octupole ones, on the gravitational bending of light. Thus, one will have to model and account for their influence while observing the sources of interest in the close proximity of some of the outer planets, notably the Jupiter and the Saturn. Results presented here are different from the ones obtained elsewhere by the fact that we specifically account for the differential nature of the future SIM astrometric campaign (e.g. observations will be made over the instrument's field of regard with the size of  $15^\circ$ ). This, in particular, lets us to obtain a more realistic estimate for the accuracy of determination of the parameterized post-Newtonian (PPN) parameter  $\gamma$ . Thus, based on a very conservative assumptions, we conclude that accuracy of  $\sigma_\gamma \sim 10^{-5}$  is achievable in the experiments conducted in the solar gravity field.

*Subject headings:* astrometry, solar system, relativity, SIM

## 1. Introduction

The last quarter of a century have changed the status of general relativity from a purely theoretical discipline to a practically important science. Present accuracy of astronomical

observations requires relativistic description of light propagation as well as the relativistically correct treatment of the dynamics of the extended celestial bodies. As a result, some of the leading static-field post-Newtonian perturbations in the dynamics of the planets, the Moon and artificial satellites have been included in the equations of motion, and in time and position transformation. Due to enormous progress in the accuracy of astronomical observations we must now study the possibility of taking into account the much smaller relativistic effects caused by the post-post-Newtonian corrections to the solar gravitational field as well as the post-Newtonian contributions from the lunar and planetary gravity. It is also well understood that effects due to non-stationary behavior of the solar system gravitational field as well as its deviation from spherical symmetry should be also considered.

Recent advances in the accuracy of astrometric observations have demonstrated importance of taking into account the relativistic effects introduced by the solar system’s gravitational environment. It is known that the reduction of the Hipparcos data has necessitated the inclusion of stellar aberration up to the terms of the second order in  $v/c$ , and the general relativistic treatment of light bending due to the gravitational field of the Sun (see discussion in Perryman et al. (1992)) and Earth (please refer to analysis in Gould (1993)). The prospect of new high precision astrometric measurements from space with the Space Interferometry Mission, will require inclusion of relativistic effects at the  $(v/c)^3$  level as shown in Turyshev & Unwin (1998). At the level of accuracy expected from SIM, even more subtle gravitational effects on astrometry from within the solar system will start to become apparent, such as the monopole and the quadrupole components of the gravitational fields of the planets and the gravito-magnetic effects caused by their motions and rotations. Thus, the identification of all possible sources of ‘astrometric’ noise that may contribute to the future SIM astrometric campaign, is well justified.

This work organized as follows: Section 2 discusses the influence of the relativistic deflection of light by the monopole components of the gravitational fields of the solar system’s bodies. We present the model and our estimates for the most important effects that will be influencing astrometric observations of a few microarcsecond ( $\mu\text{as}$ ) accuracy, that will be made from within the solar system. Section 3 will specifically address three the most intense gravitational environments in the solar system, namely the solar deflection of light and the gravitational defections in the vicinities of the Jupiter and the Earth. In Section 4 we will discuss the constraints derived from the monopole deflection of light on the navigation of the spacecraft and the accuracy of the solar system ephemerides. We study a possibility of improvement in accuracy of determination of PPN parameter  $\gamma$  via astrometric tests of general relativity in the solar system. In Section 5 we will discuss the effects of the gravitational deflection of light by the higher gravitational multipoles (both mass and current ones) of some of the bodies in the solar system. We will conclude the paper with the

discussion of the results obtained and our recommendations for future studies.

## 2. Gravity Contributions to the Local Astrometric Environment

Prediction of the gravitational deflection of light was one of the first successes of general relativity. Since the first confirmation by the Eddington expedition in 1919, the effect of gravitational deflection has been studied quite extensively and currently analysis of almost every precise astronomical measurement must take this effect into account (see Sovers & Jacobs (1996)). According to general relativity, the light rays propagating near a gravitating body are achromatically scattered by the curvature of the space-time generated by the body’s gravity field. The whole trajectory of the light ray is bent towards the body by an angle depending on the strength of the body’s gravity. The solar gravity field produces the largest effect on the light traversing the solar system.

In the PPN formalism (please refer to Will (1993)), to first order in the gravitational constant,  $G$ , the solar deflection angle  $\theta_{\text{gr}}^{\odot}$  depends only on the solar mass  $M_{\odot}$  and the impact parameter  $d$  relative to the Sun:

$$\theta_{\text{gr}}^{\odot} = \frac{1}{2}(\gamma + 1) \frac{4GM_{\odot}}{c^2 d} \frac{1 + \cos \chi}{2}. \quad (1)$$

The star is assumed to be at a very large distance compared to the Sun, and  $\chi$  is the angular separation between the deflector and the star. With the space observations carried out by SIM,  $\chi$  is not necessarily a small angle. The relevant geometry and notations are shown in Fig. 1.

The absolute magnitude for the light deflection angle is maximal for the rays grazing the solar photosphere, e.g.  $\theta_{\text{gr}}^{\odot} = \frac{1}{2}(\gamma + 1) \cdot 1.751$  mas. Most of the measurements of the gravitational deflection to date involved the solar gravity field, planets in the solar system or gravitational lenses. Thus, relativistic deflection of light has been observed, with various degrees of precision, on distance scales of  $10^9$  to  $10^{21}$  m, and on mass scales from  $10^{-3}$  to  $10^{13}$  solar masses, the upper ranges determined from the gravitational lensing of quasars (Will (1993); Dar (1992); Treuhaft & Lowe (1991)).

The parameterized post-Newtonian (PPN) parameter  $\gamma$  in the expression (1) represents the measure of the curvature of the space-time created by the unit rest mass (see Will (1993)). Note that general relativity, when analyzed in standard PPN gauge, gives:  $\gamma = 1$ . The Brans-Dicke theory is the most famous among the alternative theories of gravity. It contains, besides the metric tensor, a scalar field  $\phi$  and an arbitrary coupling constant  $\omega$ , related to this PPN parameter as  $\gamma = \frac{1+\omega}{2+\omega}$ . The present limit  $|\gamma - 1| \leq 3 \times 10^{-4}$ , that was

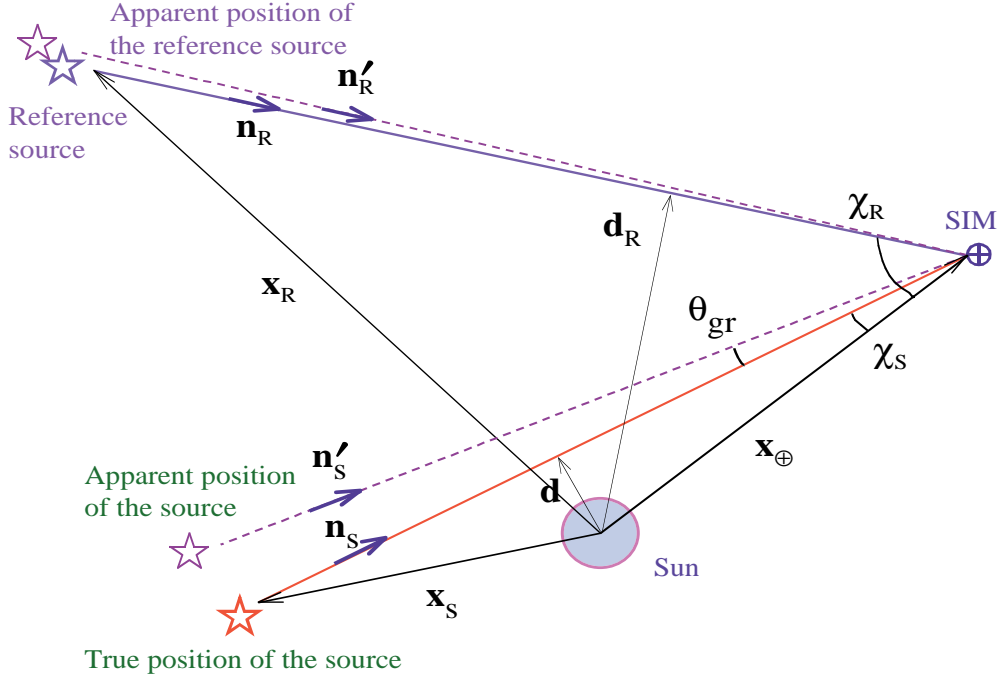


Fig. 1.— Geometry of gravitational deflection of starlight by the Sun and the planets.

recently obtained by Eubanks et al (1997), gives the constraint  $|\omega| > 3300$ .

In the Fig. 1 we emphasized the fact that the difference of the apparent position of the source from its true position depends on the impact parameter of the incoming light with respect to the deflector. For the astrometric accuracy of a few  $\mu\text{as}$  and, in the case when the Sun is the deflector, positions of all observed sources experiencing such an apparent displacement, except the ones that are on exactly opposite side from the instrument with respect to the Sun, e.g.  $\chi = \pm\pi$ . Indeed, the light rays coming from these sources do not experience gravitational deflection at all. Thus, those observations may serve as an anchor to allow one to remove the effects of the light bending from the high accuracy astrometric catalogues. This is why, in order to correctly account for the effect of gravitational deflection, it is important to process together the data taken with the different separation angles from the deflector. SIM will be observing the sky in  $15^\circ$  patches of sky, as opposed to the Very Long Baseline Interferometry (VLBI) that may simultaneously observe sources with a much larger separations on the sky. To reflect this difference, in our further estimations we will

present results for the two types of astrometric measurements, namely for the absolute (single ray deflection) and differential (two sources separated by the  $15^\circ$  field of view) observations.

## 2.1. Relativistic Deflection of Light by the Gravity Monopole

In this Section we will address the question of how the relativistic dynamics of our solar system will influence the high-precision astrometric observations with SIM. In particular, we will discuss the model, the parameterization of the quantities involved, as well as the physical meaning of the obtained contributions. The main goal of this Section is to present a comparative analysis of the various relativistic effects whose presence must be taken into account in the modeling propagation of light through the solar system. In particular we will concentrate on the effect of the relativistic deflection of light traversing our solar system’s internal gravitational environment.

### 2.1.1. Modeling the Astrometric Observations with an Interferometer

The first step into a relativistic modeling of the light path consists of determining the direction of the incoming photon as measured by an observer located in the solar system as a function of the barycentric coordinate position of the light source. Apart from second and third orders aberration the only other sizable effect is linked to the bending of light rays in the gravitational field of solar system bodies as shown by Turyshev (1998). Effects of the gravitational monopole deflection of light are the largest among those in the solar system.

In order to properly describe this gravitational light-deflecting phenomenon, one needs to define the relativistic gravity geometric contribution,  $\ell_{\text{gr}}$ , to the optical path difference (OPD) that is measurable by an interferometer in solar orbit. In a weak gravity field approximation, to first order in gravitational constant  $G$ , an additional optical path difference introduced by the gravitational bending (or, more specifically for the case of an interferometer, the gravitational delay,  $\tau_{\text{gr}}$ , see Jacobs et al (1998)) of the electromagnetic signals,  $\ell_{\text{gr}} = c\tau_{\text{gr}}$ , takes the most simple and elegant form:

$$\ell_{\text{gr}} = -(\gamma + 1) \sum_B \frac{G M_B}{c^2 r_B} \left[ \frac{\vec{b}(\vec{s} + \vec{n}_B)}{1 + (\vec{s} \cdot \vec{n}_B)} \right], \quad (2)$$

where  $r_B$  is the distance from SIM to a deflecting body  $B$ ,  $\vec{n}_B$  is the unit vector in this direction. Also  $\vec{b} = b\vec{n}$  and  $\vec{s}$  are the vector of interferometer’s baseline and the unit vector of the unperturbed direction to the source at infinity correspondingly. Note that Eq.(2) is

written in the approximation neglecting the terms of the order  $\sim M_B b^2 / r_B^2$ , which could be reinstated, if needed.

For the purposes of this study it is sufficient to confine our analysis to a planar motion and parameterize the quantities involved as follows:

$$\vec{b} = b(\cos \epsilon, \sin \epsilon), \quad \vec{r}_B = r_B(\cos \alpha_B, \sin \alpha_B), \quad \vec{s} = (\cos \theta, \sin \theta), \quad (3)$$

where  $\epsilon$  is the angle of the baseline's orientation with respect to the instantaneous body-centric coordinate frame,  $\alpha_B$  is the right ascension angle of the interferometer as seen from the this frame and  $\theta$  is the direction to the observed source correspondingly. The geometry of the problem and the discussed notations are presented in the Figure 2. It is convenient

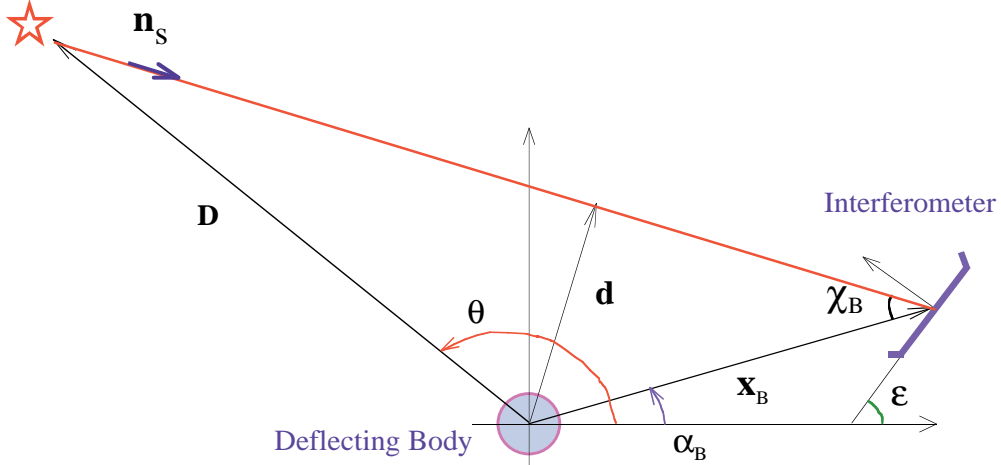


Fig. 2.— Parameterization and notations for the gravitational deflection of light.

to express the gravitational contribution to the total optical path difference Eq.(2) in terms of the deflector and the source separation angle  $\chi_B$  as observed by the interferometer. The necessary relation that expresses the source's position angle  $\theta$  via the separation angle  $\chi_B$  may be given as:

$$\theta = \pi + \alpha_B - \chi_B - \arcsin \left[ \frac{r_B}{D} \sin \chi_B \right]. \quad (4)$$

As a result, we can now rewrite the gravitational deflection's contribution to the total OPD,

Eq.(2), in the following form:

$$\ell_{\text{gr}} = -(\gamma + 1) \sum_B \frac{G M_B b}{c^2 r_B} \left[ \cos(\epsilon - \alpha_B) + \sin(\epsilon - \alpha_B) \frac{1 + \cos \chi_B^*}{\sin \chi_B^*} \right], \quad (5)$$

where  $\chi_B^* = \chi_B + \arcsin \left[ \frac{r_B}{D} \sin \chi_B \right]$ . We can further assume that the source is located at a very large distance,  $D$ , compare to the distance between the interferometer and the deflector, so that the following inequality holds  $r_B \ll D$  for every body in the solar system. This allows us to neglect the presence of the last term in the equation Eq.(4) for the estimation purposes only. Also a complete analysis of phenomenon of the gravitational deflection of light will have to account for the time dependency in all the quantities involved. Thus, one will have to use the knowledge of the position of the spacecraft in the solar system's barycentric reference frame, the instrument's orientation in the proper coordinate frame, the time that was spent in a particular orientation, the history of all the maneuvers and re-pointings of the instrument, etc. These issues are closely related to the principles of the operational mode of the instrument that is currently still being developed.

### 2.1.2. Modeling for the Absolute Astrometric Observations

Equation Eq.(5) represents the fact that the gravitational field is affecting the propagation of the electromagnetic signals in a two ways, namely by delaying them and by deflecting the light's trajectory from the rectilinear one. Thus, the first term in the square brackets on the right hand-side of this equation is the term that describes the gravitational delay of the infallen electromagnetic signal. This term is independent on the source's position on the sky and depends only on the orientation of the baseline vector and the direction to the deflector. More precisely, it depends on the gravity generated by the body at the interferometer's location and the projected baseline vector onto the direction to the source ( $\vec{b} \cdot \vec{n}_B = b \cos(\epsilon - \alpha_B)$ ). For the purposes of this study it is sufficient to discuss only the magnitude of this effect in terms of its contribution to the astrometric measurement:

$$\theta_{\text{gr}}^{\text{delay}} = \frac{\ell_{\text{gr}}^{\text{delay}}}{b} = -(\gamma + 1) \sum_B \frac{G M_B}{c^2 r_B}. \quad (6)$$

The second term in the equation Eq.(5) is responsible for the relativistic deflection of light and will be the main topic of our further discussion. In our future analysis we will be interested only in magnitudes of the angles of relativistic deflection of light, so it is convenient to choose [only for the estimation purposes!] such an orientation of the baseline vector (e.g. angle  $\epsilon$ ) and the vector of mutual orientation of the instrument and the deflecting body (e.g.

angle  $\alpha_B$ ) that maximizes the effect of the gravitational deflection of light. By choosing the orientation angles as  $\epsilon - \alpha_B = \frac{\pi}{2}$ , we can neglect its presence. This allows one to concentrate only on the phenomenon of the gravitational deflection and to re-write the contribution of this effect to the total OPD, Eq.(5), as  $\ell_{\text{gr}} = -\sum_B \ell_{\text{gr}}^B$ , with individual contributions  $\ell_{\text{gr}}^B$  given by

$$\ell_{\text{gr}}^B = (\gamma + 1) \frac{G M_B b}{c^2 r_B} \frac{1 + \cos \chi_B}{\sin \chi_B}. \quad (7)$$

It is also convenient to express this additional OPD in terms of the corresponding deflection angles  $\theta_{\text{gr}}^B$ , which simply have the form:

$$\theta_{\text{gr}}^B = \frac{\ell_{\text{gr}}^B}{b} = (\gamma + 1) \frac{G M_B}{c^2 r_B} \frac{1 + \cos \chi_B}{\sin \chi_B}. \quad (8)$$

Note that  $r_B \sin \chi_B = d_B$  is the impact parameter of the incident light ray with respect to a particular deflector as seen by the interferometer. By substituting this result into the formula (7) one obtains an expression similar to that given by Eq.(1).

The obtained expressions Eqs.(7)-(8) are most appropriate to estimate the magnitude of the gravitational bending effects introduced into absolute astrometric measurements. They are useful in understanding the ‘‘asymptotic value’’ of the effect for a large number of observations,  $N \gg 1$ . However, one needs an additional set of equations suitable to describe the accuracy of measurements during differential astrometry studies with SIM.

### 2.1.3. Differential Astrometric Measurements

The necessary expression for the differential OPD may be simply obtained by subtracting OPDs for the different sources one from another. This procedure resulted in the following expression:

$$\delta \ell_{\text{gr}}^B = \ell_{1\text{gr}}^B - \ell_{2\text{gr}}^B = -(\gamma + 1) \sum_B \frac{G M_B}{c^2 r_B} \left[ \frac{\vec{b}(\vec{s}_1 + \vec{n}_B)}{1 + (\vec{s}_1 \vec{n}_B)} - \frac{\vec{b}(\vec{s}_2 + \vec{n}_B)}{1 + (\vec{s}_2 \vec{n}_B)} \right], \quad (9)$$

where  $\vec{s}_1$  and  $\vec{s}_2$  are the barycentric positions of the primary and the secondary objects. By using parameterization for the quantities involved similar to that above, this expression may be presented in terms of the deflector-source separation angles,  $\chi_{1B}$ ,  $\chi_{2B}$ , as follows:

$$\delta \ell_{\text{gr}} = -(\gamma + 1) \sum_B \frac{G M_B b}{c^2 r_B} \sin(\epsilon - \alpha_B) \frac{\sin \frac{1}{2}(\chi_{B2} - \chi_{B1})}{\sin \frac{1}{2}\chi_{B1} \sin \frac{1}{2}\chi_{B2}}. \quad (10)$$



The purpose of this was only to estimate the influence of the solar system’s gravity field on the propagation of light. We will concentrate on obtaining the magnitudes of the deflection angles only and will not try to reconstruct the complicated functional dependency of the effect on the number of mutual orientation angles. This allows us use the expression Eq.(10) with such an orientation between the baseline vector,  $\epsilon$ , and deflector\_instrument angle,  $\alpha_B$ , that maximizes contribution of each individual deflector for a particular orbital position of the spacecraft. As a result, we may well require that  $\epsilon - \alpha_B = \frac{\pi}{2}$  and expression Eq.(10) may be re-written as  $\delta\ell_{\text{gr}} = -\sum_B \delta\ell_{\text{gr}}^B$ , with the individual contributions  $\delta\ell_{\text{gr}}^B$  having the form

$$\delta\ell_{\text{gr}}^B = (\gamma + 1) \frac{G M_B b}{c^2 r_B} \frac{\sin \frac{1}{2}(\chi_{2B} - \chi_{1B})}{\sin \frac{1}{2}\chi_{1B} \cdot \sin \frac{1}{2}\chi_{2B}}. \quad (11)$$

Finally, it is convenient to express this result for  $\delta\ell_{\text{gr}}^B$  in terms of the corresponding deflection angle  $\delta\theta_{\text{gr}}$ . Similarly to the expression Eq.(8), one obtains:

$$\delta\theta_{\text{gr}}^B = \frac{\delta\ell_{\text{gr}}^B}{b} = (\gamma + 1) \frac{G M_B}{c^2 r_B} \frac{\sin \frac{1}{2}(\chi_{2B} - \chi_{1B})}{\sin \frac{1}{2}\chi_{1B} \cdot \sin \frac{1}{2}\chi_{2B}}. \quad (12)$$

#### 2.1.4. Deflection of Grazing Rays by the Bodies of the Solar System

In this section we will obtain the estimates for the effects that characterize the intensity of the gravitational environment in the solar system. The most natural and convenient way to do that is to discuss the magnitudes of the angles of the gravitational deflection of light rays that grazing the surfaces of the celestial bodies.

In the two previous sections we have obtained expressions suitable to describe effects of the gravitational bending of light on both absolute and differential astrometric observations. Now we have all that is necessary to estimate the influence of the solar system’s gravity field on the future high-accuracy astrometric observations. The corresponding post-Newtonian effects for grazing rays, deflected by the solar system’s bodies, are given in the Table 1. To obtain these estimates we used the physical constants and the solar system’s parameters that are given in the Tables 16 and 17. The results presented in the terms of the following quantities:

- i). for the absolute astrometry we present the results in terms of the absolute measurements  $\ell_{\text{gr}}^B, \theta_{\text{gr}}^B$  defined by Eq.(7) and Eq.(8);
- ii). to describe the differential observations we use the relations Eq.(11) and Eq.(12) and express those in terms of the differential astrometric observables, namely  $\delta\ell_{\text{gr}}^B, \delta\theta_{\text{gr}}^B$ .

Table 1: Relativistic monopole deflection of grazing (e.g.  $\chi_{1B} = \mathcal{R}_B$ ) light rays by the bodies of the solar system at the SIM’s location that is assumed to be placed in the solar Earth-trailing orbit. For the differential observations the two stars are assumed to be separated by the size of the instrument’s field of regard. For the grazing rays, position of the primary star is assumed to be on the limb of the deflector. Moreover, results are given for the smallest distances from SIM to the bodies (e.g. when the gravitational deflection effect is largest). For the Earth-Moon system we took the SIM’s position at the end of the first half of the first year mission at the distance of 0.05 AU from the Earth. Presented in the right column of this Table are the magnitudes of the body’s individual contributions to the gravitational delay of light at the SIM’s location (note that it is unobservable in the case of differential astrometry with SIM).

Solar system’s object	Angular size from SIM, $\mathcal{R}_B$ , arcsec	Deflection of grazing rays			Delay $\theta_{\text{gr}B}^{\text{delay}}$ , $\mu\text{as}$
		absolute $\theta_{\text{gr}}^B$ , $\mu\text{as}$	diff. [15°] $\delta\theta_{\text{gr}}^B$ , $\mu\text{as}$	diff. [1°] $\delta\theta_{\text{gr}}^B$ , $\mu\text{as}$	
Sun	0°.26656	1".75064	1".72025	1".38221	4072.29
Sun at 45°	45°	9,831.39	2,777.97	237.66	-same-
Moon	47.92690	25.91	25.87	25.56	0.003
Mercury	5.48682	82.93	82.92	82.81	0.001
Venus	30.15040	492.97	492.69	488.88	0.036
Earth	175.88401	573.75	571.90	547.03	0.245
Mars	8.93571	115.85	115.83	115.57	0.003
Jupiter	23.23850	16,419.61	16,412.60	16,314.30	0.925
Jupiter at 30"	30.0	12,719.12	12,712.03	12,614.21	-same-
Saturn	9.64159	5,805.31	5,804.27	5,789.79	0.126
Uranus	1.86211	2,171.38	2,171.30	2,170.26	0.010
Neptune	1.18527	2,500.35	2,500.29	2,499.52	0.007
Pluto	0.11478	2.82	2.82	2.82	0.00

Note, that the angular separation of the secondary star will always be taken larger than that for the primary. It is convenient to study the case of the most distant available separations of the sources. In the case of SIM, this is the size of the field of regard (FoR). Thus for the wide-angle astrometry the size of FoR will be  $15^\circ \equiv \frac{\pi}{12}$ , thus  $\chi_{2B} = \chi_{1B} + \frac{\pi}{12}$ . For the narrow-angle observations this size is  $\text{FoR} = 1^\circ \equiv \frac{\pi}{180}$ , thus for this type of astrometric observations we will use  $\chi_{2B} = \chi_{1B} + \frac{\pi}{180}$ . Additionally, the baseline length will be assumed  $b = 10$  m.

In the Table 1 we also presented the magnitudes of the individual solar and planetary contributions to the total gravitational delay of light traversing the solar system at the SIM's location,  $\theta_{\text{gr}B}^{\text{delay}}$ . This contribution is given by Eq.(6) and it affects only the absolute astrometric measurements. Thus, one may see that it is important to account for this effect only in case of gravity contributions of the Sun and the Jupiter only.

## 2.2. Critical Impact Parameter for High Accuracy Astrometry

The estimates, presented in the Table 1 have demonstrated that it is very important to correctly model and account for gravitational influence of the bodies of the solar system. Depending on the impact parameter  $d_B$  (or planet-source separation angle,  $\chi_B$ ), one will have to account for the post-Newtonian deflection of light by a particular planet. Most important is that one will have to permanently monitor the presence of some of the bodies of the solar system during all astrometric observations, independently on the position of the spacecraft in it's solar orbit and the observing direction. The bodies that introduce the biggest astrometric inhomogeneity are the Sun, the Jupiter and the Earth (especially at the beginning of the mission, when the spacecraft is in the Earth' immediate proximity).

Let us introduce a measure of such a gravitational inhomogeneity due to a particular body in the solar system. To do this, suppose that future astrometric experiments with SIM will be capable to measure astrometric parameters with accuracy of  $\Delta\theta_0 = \Delta k \mu\text{as}$ , where  $\Delta k$  is some number characterizing the accuracy of the instrument [e.g. for a single measurement accuracy  $\Delta k = 8$  and for the mission accuracy  $\Delta k = 4$ ]. Then, there will be a critical distance from the body, beginning from which, it is important to account for the presence of the body's gravity in the vicinity of the observed part of the sky. Let's call this distance — critical impact parameter,  $d_{\text{crit}}^B$ , the closest distance between the body and the light ray that is gravitationally deflected to the angle

$$\theta_{\text{gr}}^c(d_{\text{crit}}^B) = \Delta\theta_0 = \Delta k \mu\text{as}. \quad (13)$$

The necessary expression for  $d_c^B$  may be obtained with the help of Eq.(8) as follows:

$$d_{\text{crit}}^B = \pm \frac{4\mu_B}{\Delta\theta_0} \left[ 1 + \left( \frac{2\mu_B}{\Delta\theta_0 r_B} \right)^2 \right]^{-1}, \quad (14)$$

where  $\mu_B = c^{-2}GM_B$  is the usual notation for the gravitational ( $\frac{1}{2}$ Schwarzschild) radius of the body. The choice of the sign depends on the relation between the terms, thus if  $4\mu_B/r_B > \Delta\theta_0$ , then the negative sign should be chosen. The negative sign reflects the fact that the impact parameter becomes critical [e.g. satisfies the equation Eq.(13)] for the sources that have the deflector-source separation angle on the sky  $|\chi_B|$  more than  $90^\circ$ . This is definitely true for the case of accounting for gravitational influence of the two solar system bodies, namely the Sun and the Jupiter. For the other bodies of the solar system the ratio holds as  $4\mu_B/r_B \ll \Delta\theta_0 = \text{few } \mu\text{as}$ , thus significantly simplifying the analytical expression Eq.(14).

The formula for the critical distance, Eq.(14), may be given in a slightly different form, representing the critical angles,  $\alpha_c^B$ , that correspond to this critical distance from the body:

$$\alpha_c^B = \arcsin \left( \frac{d_{\text{crit}}^B}{r_B} \right) = \arcsin \left[ \frac{4\mu_B}{\Delta\theta_0 r_B} \left[ 1 + \left( \frac{2\mu_B}{\Delta\theta_0 r_B} \right)^2 \right]^{-1} \right]. \quad (15)$$

Different forms of the critical impact parameters  $d_{\text{crit}}^B$  for  $\Delta k = 1$  are given in the Table 2. With the help of Eq.(14), the results given in this table are easily scaled for any astrometric accuracy  $\Delta k$ .

### 2.3. Deflection of Light by Planetary Satellites

One may expect that the planetary satellites will affect the astrometric studies a light ray would pass in their vicinities. Just for completeness of our study we would like to present the estimates for the gravitational deflection of light by the planetary satellites and the small bodies in the solar system. The corresponding estimates for deflection angles,  $\theta_{\text{gr}}^B$ , and critical distances,  $d_{\text{crit}}$  are presented in the Table 3. Due, to the fact that the angular sizes for those bodies are much less than the smallest field of regard of the SIM instrument (e.g. FoR= $1^\circ$ ), the results for the differential observations will be effectively insensitive to the size of the the two available FoRs. The obtained results demonstrate the fact that observations of of these objects with that size of FoR will evidently have the effect from the relativistic bending of light. Thus, we have presented there only the angle for the absolute gravitational deflection in terms of quantities  $\theta_{\text{gr}}^B$ . As a result, the major satellites of Jupiter, Saturn and Neptune should also be included in the model if the light ray passes close to these bodies.

Table 2: Relativistic monopole deflection of light: the angles and the critical distances for  $\Delta\theta_0 = 1 \mu\text{as}$  astrometric accuracy. Negative critical distance for the Sun represents the fact that the Sun-source critical separation angle,  $\alpha_c^B$ , is larger than  $90^\circ$ . To visualize the solar gravitational deflection power note that a light ray coming perpendicular to the ecliptic plane at the distance of  $d_{1\mu\text{as}} = 4072.3 \text{ AU}$  from the Sun will be still deflected by the solar gravity to  $1 \mu\text{as}$ ! The critical distances for the Earth are given for two distances, namely for  $0.05 \text{ AU}$  ( $27^\circ.49$ ) and  $0.01 \text{ AU}$  ( $78^\circ.54$ ).

Object	$\theta_{\text{gr}}^B, \mu\text{as}$	Critical distances for accuracy of $1 \mu\text{as}$		
		$d_{\text{crit}}^B, \text{cm}$	$d_{\text{crit}}^B, \text{deg}$	$d_{\text{crit}}^B, \mathcal{R}_B$
Sun	$1''.75064$	$-7.347 \times 10^9$	$\pi + 101''.3$	$0.11 \cdot \mathcal{R}_\odot$
Moon	25.91	$4.501 \times 10^9$	$0^\circ.34 - 1^\circ.72$	$25.9 \cdot \mathcal{R}_m$
Mercury	82.93	$2.023 \times 10^{10}$	$0^\circ.06 - 0^\circ.13$	$82.9 \cdot \mathcal{R}_{Me}$
Venus	492.97	$2.982 \times 10^{11}$	$0^\circ.66 - 4^\circ.13$	$492.9 \cdot \mathcal{R}_V$
Earth	573.75	$3.453 \times 10^{11}$	$27^\circ.49 - 78^\circ.54$	$541.4 \cdot \mathcal{R}_\oplus$
Mars	115.85	$3.931 \times 10^{10}$	$0^\circ.06 - 0^\circ.29$	$115.9 \cdot \mathcal{R}_{Ms}$
Jupiter	16,419.61	$6.270 \times 10^{13}$	$64^\circ.06 - 88^\circ.51$	$8,849 \cdot \mathcal{R}_J$
Saturn	5,805.31	$3.420 \times 10^{13}$	$12^\circ.56 - 15^\circ.45$	$5,700 \cdot \mathcal{R}_S$
Uranus	2,171.38	$5.319 \times 10^{12}$	$1^\circ.01 - 1^\circ.12$	$2,171 \cdot \mathcal{R}_U$
Neptune	2,500.35	$6.276 \times 10^{12}$	$0^\circ.77 - 0^\circ.82$	$2,500 \cdot \mathcal{R}_N$
Pluto	2.82	$9.025 \times 10^8$	$0''.31 - 0''.32$	$2.8 \cdot \mathcal{R}_P$

Table 3: Relativistic deflection of light by some planetary satellites.

Object	Mass, $10^{25} \text{ g}$	Radius, $\mathcal{R}_B, \text{km}$	Angular size, $\mathcal{R}_B, \text{arcsec}$	Grazing $\theta_{\text{gr}}^B, \mu\text{as}$	1 $\mu\text{as}$ critical radius	
					$d_{\text{crit}}, \text{km}$	$d_{\text{crit}}, \mathcal{R}_{\text{planet}}$
Io	7.23	1,738	0.570056	25.48	44,291	$0.63 \cdot \mathcal{R}_J$
Europa	4.7	1,620	0.531353	17.77	28,793	$0.41 \cdot \mathcal{R}_J$
Ganymede	15.5	1,415	0.464114	67.11	94,954	$1.34 \cdot \mathcal{R}_J$
Callisto	9.66	2,450	0.803589	24.15	59,178	$0.84 \cdot \mathcal{R}_J$
Rhea	0.227	675	0.108468	2.06	1,391	$0.02 \cdot \mathcal{R}_S$
Titan	14.1	2,475	0.397715	34.90	86,378	$1.44 \cdot \mathcal{R}_S$
Triton	13	1,750	0.082638	45.51	79,639	$3.17 \cdot \mathcal{R}_N$

### 2.4. Gravitational Influence of Small Bodies

Additionally, for  $\Delta k$   $\mu\text{as}$  astrometric accuracy, one needs to account for the post-Newtonian deflection of light due to rather a large number of small bodies in the solar system having a mean radius

$$\mathcal{R}_B \geq 624 \sqrt{\frac{\Delta k}{\rho_B}} \text{ km.} \tag{16}$$

The deflection angle for the largest asteroids Ceres, Pallas and Vesta for  $\Delta k = 1$  are given in the Table 4. The quoted properties of the asteroids were taken from Standish & Hellings (1989). Positions of these asteroids are known and they are incorporated in the JPL ephemerides. However, due to the fact that the other small bodies (e.g. asteroids, Kuiper belt objects, etc.) may produce a stochastic noise in the future astrometric observations with SIM, so they should also be properly modeled.

Table 4: Relativistic deflection of light by the asteroids.

Object	$\rho_B$ , g/cm <sup>3</sup>	Radius, km	$\theta_{\text{gr}}^B$ , $\mu\text{as}$
Ceres	2.3	470	1.3
Pallas	3.4	269	0.6
Vesta	3.6	263	0.6
Class S	$2.1 \pm 0.2$	TBD	$\leq 0.3$
Class C	$1.7 \pm 0.5$	TBD	$\leq 0.3$

## 3. Most Gravitationally Intense Astrometric Regions for SIM

The properties of the solar system’s gravity field presented in the Tables 1 and 2 suggesting that the most intense gravitational environments in the solar system are those offered by the Sun and two planets, namely the Earth and the Jupiter. In this Section we will analyze these regions in a more details.

### 3.1. Gravitational Deflection of Light by the Sun

From the expressions Eq.(8) and Eq.(12) we obtain the relations for relativistic deflection of light by the solar gravitational monopole. The expression for the absolute astrometry takes

the form:

$$\theta_{\text{gr}}^{\odot} = (\gamma + 1) \frac{G M_{\odot}}{c^2 r_{\odot}} \frac{1 + \cos \chi_{1\odot}}{\sin \chi_{1\odot}} = 4.072 \cdot \frac{1 + \cos \chi_{1\odot}}{\sin \chi_{1\odot}} \quad \text{mas}, \quad (17)$$

where  $\chi_{1\odot}$  is the Sun-source separation angle,  $r_{\odot} = 1$  AU, and  $\gamma = 1$ . Similarly, for differential astrometric observations one obtains:

$$\delta\theta_{\text{gr}}^{\odot} = (\gamma + 1) \frac{G M_{\odot}}{c^2} \frac{\sin \frac{1}{2}(\chi_{2\odot} - \chi_{1\odot})}{r_{\odot} \sin \frac{1}{2}\chi_{1\odot} \cdot \sin \frac{1}{2}\chi_{2\odot}} = 4.072 \cdot \frac{\sin \frac{1}{2}(\chi_{2\odot} - \chi_{1\odot})}{\sin \frac{1}{2}\chi_{1\odot} \cdot \sin \frac{1}{2}\chi_{2\odot}} \quad \text{mas}, \quad (18)$$

with  $\chi_{1\odot}, \chi_{2\odot}$  being the Sun-source separation angles for the primary and the secondary stars correspondingly. Remember that we use the two stars separated by the SIM's field of regard, namely  $\chi_{2\odot} = \chi_{1\odot} + \frac{\pi}{12}$ . The solar angular dimensions from the Earth' orbit are calculated to be  $\mathcal{R}_{\odot} = 0^{\circ}.26656$ . This angle corresponds to a deflection of light to 1.75065 arcsec on the limb of the Sun. Results for the most interesting range of  $\chi_{1\odot}$  are given in the Table 5.

A qualitative presentation of the solar gravitational deflection is given in the Figure 3. The upper thick line on both plots represents the absolute astrometric measurements, while the other two are for the differential astrometry. Thus, the middle dashed line is for the observations over the maximal field of regard of the instrument FoR = 15°, the lower thick line is for FoR = 1°.

### 3.1.1. Second Order Post-Newtonian Effects in the Solar Deflection

One may also want to account for the post-post-Newtonian (post-PN) terms (e.g.  $\propto G^2$ ) as well as the contributions due to other PPN parameters (refer to Will (1993)). Thus, in the weak gravity field approximation the total deflection angle  $\theta_{\text{gr}}$  has an additional contribution due the post-post-Newtonian terms in the metric tensor. For the crude estimation purposes this effect could be given by the following expression:

$$\delta\theta_{\text{post-PN}} = \frac{1}{4}(\gamma + 1)^2 \left( \frac{2GM}{c^2 d} \right)^2 \left( \frac{15\pi}{16} - 1 \right) \left( \frac{1 + \cos \chi}{2} \right)^2. \quad (19)$$

However, a quick look on the magnitudes of these terms for the solar system's bodies suggested that SIM astrometric data will be insensitive to the post-PN effects. The post-PN effects due to the Sun are the largest among those in the solar system. However, even for the absolute astrometry with the Sun-grazing rays the post-PN terms were estimated to be of order  $\delta\theta_{\text{post-PN}}^{\odot} = 7 \mu\text{as}$  (see Turyshev (1998)). Note that the SIM solar avoidance angle (SAA) is constraining the Sun-source separation angle as  $\chi_{1\odot} \geq 45^{\circ}$ . The post-PN effect

Table 5: Magnitudes of the gravitational deflection angle vs. the Sun-source separation angle  $\chi_{1\odot}$ .

Solar deflection	small $\chi_{1\odot}$ , deg						
	0°.27	0°.5	1°	2°	5°	10°	15°
$\theta_{\text{gr}}^{\odot}$ , mas	1,728	933.295	466.639	233.302	93.271	46.547	30.932
$\delta\theta_{\text{gr}}^{\odot}$ [15°], mas	1,698	903.372	437.663	206.053	70.176	28.178	15.734
$\delta\theta_{\text{gr}}^{\odot}$ [1°], mas	1,361	622.212	233.337	77.787	15.567	4.254	1.956

Solar deflection	large $\chi_{1\odot}$ , deg							
	20°	40°	45°	50°	60°	70°	80°	90°
$\theta_{\text{gr}}^{\odot}$ , mas	23.095	11.189	9.832	8.733	7.053	5.816	4.853	4.072
$\delta\theta_{\text{gr}}^{\odot}$ [15°], mas	10.180	3.366	2.778	2.341	1.746	1.372	1.122	0.948
$\delta\theta_{\text{gr}}^{\odot}$ [1°], mas	1.123	0.297	0.238	0.195	0.140	0.107	0.085	0.071

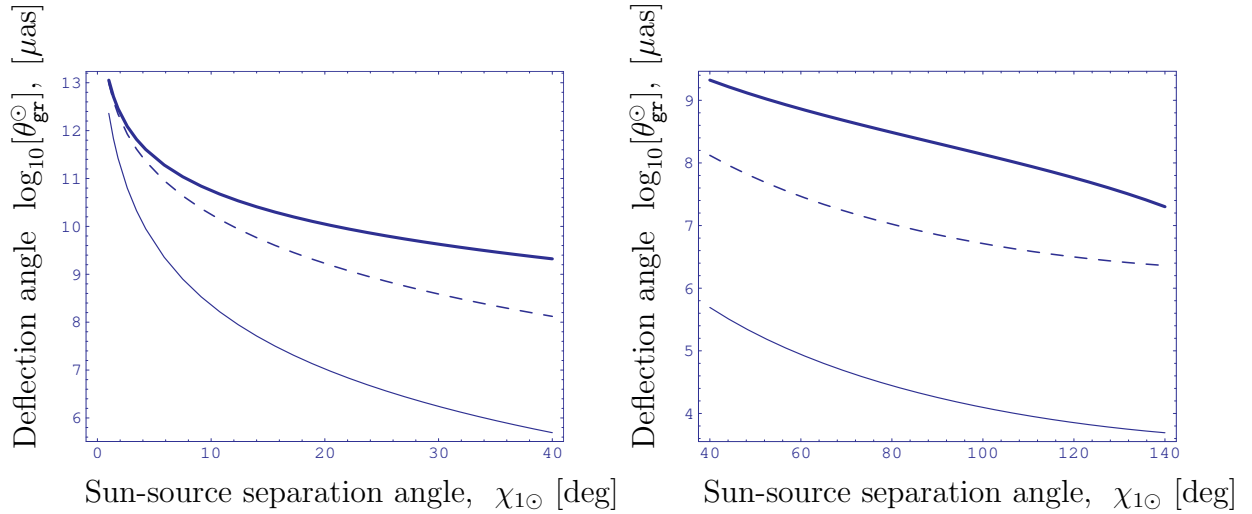


Fig. 3.— Solar gravitational deflection of light. On all plots: the upper thick line is for the absolute astrometric measurements, while the other two are for the differential astrometry. Thus, the dashed line is for the observations over field of regard of FoR = 15°, the lower thick line is for FoR = 1°.



is inversely proportional to the square of the impact parameter, thus reducing the effect to  $\delta\theta_{\text{post-PN}}^{\odot} \leq 3.1$  nanoarcseconds on the rim of SAA. This is why the post-PN effects will not be accessible with SIM.

### 3.2. Gravitational Deflection of Light by the Jupiter

One may obtain the expression, similar to Eq.(17) for the relativistic deflection of light by the Jovian gravitational monopole in the following form:

$$\theta_{\text{gr}}^J = (\gamma + 1) \frac{G M_J}{c^2 r_J} \frac{1 + \cos \chi_{1J}}{\sin \chi_{1J}} = 0.924944 \cdot \frac{1 + \cos \chi_{1J}}{\sin \chi_{1J}} \quad \mu\text{as}, \quad (20)$$

with  $\chi_{1J}$  being the Jupiter-source separation angle as seen by the interferometer at the distance  $r_J$  from the Jupiter. For the differential observations one will have expression, similar to that Eq.(18) for the Sun:

$$\delta\theta_{\text{gr}}^J = (\gamma + 1) \frac{G M_J}{c^2 r_J} \frac{\sin \frac{1}{2}(\chi_{2J} - \chi_{1J})}{\sin \frac{1}{2}\chi_{1J} \cdot \sin \frac{1}{2}\chi_{2J}} = 0.924944 \cdot \frac{\sin \frac{1}{2}(\chi_{2J} - \chi_{1J})}{\sin \frac{1}{2}\chi_{1J} \cdot \sin \frac{1}{2}\chi_{2J}} \quad \mu\text{as}, \quad (21)$$

where again  $\chi_{1J}, \chi_{2J}$  are the Jupiter-source separation angles for the primary and secondary stars correspondingly,  $\chi_{2J} = \chi_{1J} + \frac{\pi}{12}$  (and  $\chi_{2J} = \chi_{1J} + \frac{\pi}{180}$  for the narrow angle astrometry). The largest effect will come when SIM and the Jupiter are at the closest distance from each other  $\sim 4.2$  AU. The Jupiter's angular dimensions from the Earth' orbit for this situation are calculated to be  $\mathcal{R}_J = 23.24$  arcsec, which correspond to a deflection angle of 16.419 mas. Results for some  $\chi_{1J}$  are given in the Table 6. Note that for the light rays coming perpendicular to the ecliptic plane the Jovian deflection will be in the range:  $\delta\alpha_{1J} \sim (0.7 - 1.0) \mu\text{as}$ !

A qualitative behavior of the effect of the gravitational deflection of light by the Jovian gravity field is plotted in the Figure 4. As in the case of the solar deflection, the upper thick line on both plots represents the absolute astrometric measurements, while the other two are for the differential astrometry (the dashed line is for the observations over FoR = 15° and the lower thick line is for FoR = 1°).

### 3.3. Gravitational Deflection of Light by the Earth

The deflection of light rays by the Earth's gravity field may also be of interest. The expressions, describing the relativistic deflection of light by the Earth' gravitational monopole

Jovian deflection	Jupiter-source separation angles $\chi_{1J}$ , arcsec							
	23.24''	26''	30''	60''	120''	180''	360''	90°
$\theta_{\text{gr}}^J$ , mas	16.419	14.676	12.719	6.360	3.180	2.120	1.060	0.9 $\mu\text{as}$
$\delta\theta_{\text{gr}}^J [15^\circ]$ , mas	16.412	14.669	12.712	6.352	3.173	2.113	1.053	0.2 $\mu\text{as}$
$\delta\theta_{\text{gr}}^J [1^\circ]$ , mas	16.313	14.570	12.614	6.255	3.077	2.019	0.964	0.0 $\mu\text{as}$

Table 6: Jovian gravitational monopole deflection vs. the Jupiter-source sky separation angle  $\chi_{1J}$ .

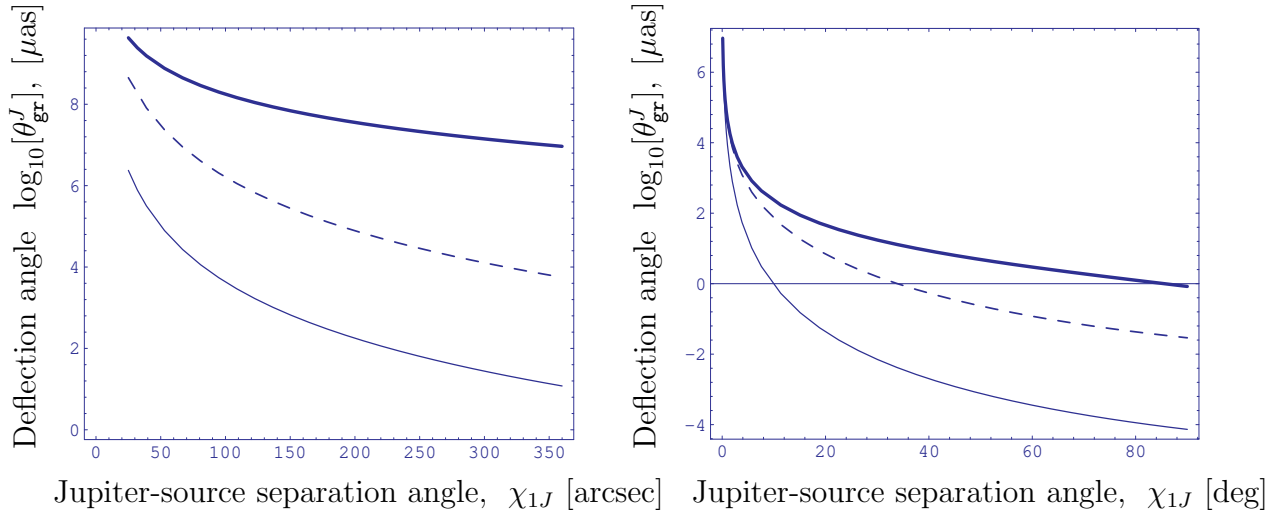


Fig. 4.— Jovian gravitational deflection of light.

are given below:

$$\theta_{\text{gr}}^{\oplus} = (\gamma + 1) \frac{G M_{\oplus}}{c^2 r_{\oplus}} \frac{1 + \cos \chi_{1\oplus}}{\sin \chi_{1\oplus}} = 0.2446 \cdot \frac{1 + \cos \chi_{1\oplus}}{\sin \chi_{1\oplus}} \mu\text{as}, \quad (22)$$

with  $\chi_{1\oplus}$  being the Earth-source separation angle as seen by the interferometer at the distance  $r_{\odot}$  from the Earth. Relation for the differential astrometric measurements was obtained in the form:

$$\delta\theta_{\text{gr}}^{\oplus} = (\gamma + 1) \frac{G}{c^2} \frac{M_{\oplus}}{r_{\oplus}} \frac{\sin \frac{1}{2}(\chi_{2\oplus} - \chi_{1\oplus})}{\sin \frac{1}{2}\chi_{1\oplus} \cdot \sin \frac{1}{2}\chi_{2\oplus}} = 0.2446 \cdot \frac{\sin \frac{1}{2}(\chi_{2\oplus} - \chi_{1\oplus})}{\sin \frac{1}{2}\chi_{1\oplus} \cdot \sin \frac{1}{2}\chi_{2\oplus}} \mu\text{as}, \quad (23)$$

where, as before,  $\chi_{1\oplus}, \chi_{2\oplus}$  are the Earth-source separation angles for the primary and secondary stars correspondingly,  $\chi_{2\oplus} = \chi_{1\oplus} + \frac{\pi}{12}$  (and  $\chi_{2\oplus} = \chi_{1\oplus} + \frac{\pi}{180}$  for the narrow angle

astrometry). The largest effect will come when SIM and the Earth are at the closest distance, say at the end of the first half of the first year of the mission,  $r_{\oplus} = 0.05$  AU. The Earth’s angular dimensions being measured from the spacecraft from that distance are calculated to be  $\mathcal{R}_{\oplus}^{\text{SIM}} = 175.88401$  arcsec, which correspond to a deflection angle of  $573.75 \mu\text{as}$ . The deflection angles for a few  $\chi_{1\oplus}$  are given in the Table 7.

Table 7: Solar relativistic deflection angle as a function of the Earth-source separation angle  $\chi_{1\oplus}$ . Results for SIM are given for the first half of the first year mission, when the distance between the spacecraft and the Earth is  $\sim 0.05$  AU.

SIM mission	$\chi_{1\oplus}^{\text{SIM}}$ , arcsec						
	175.88	200	360	1°	5°	10°	15°
$\theta_{1\oplus}$ , $\mu\text{as}$	573.8	504.7	280.3	28.0	5.6	2.8	1.9
$\delta\theta_{1\oplus}[15^\circ]$ , $\mu\text{as}$	571.9	502.7	278.5	26.3	4.2	1.7	1.0
$\delta\theta_{1\oplus}[1^\circ]$ , $\mu\text{as}$	547.0	478.0	254.8	14.0	0.9	0.3	0.1

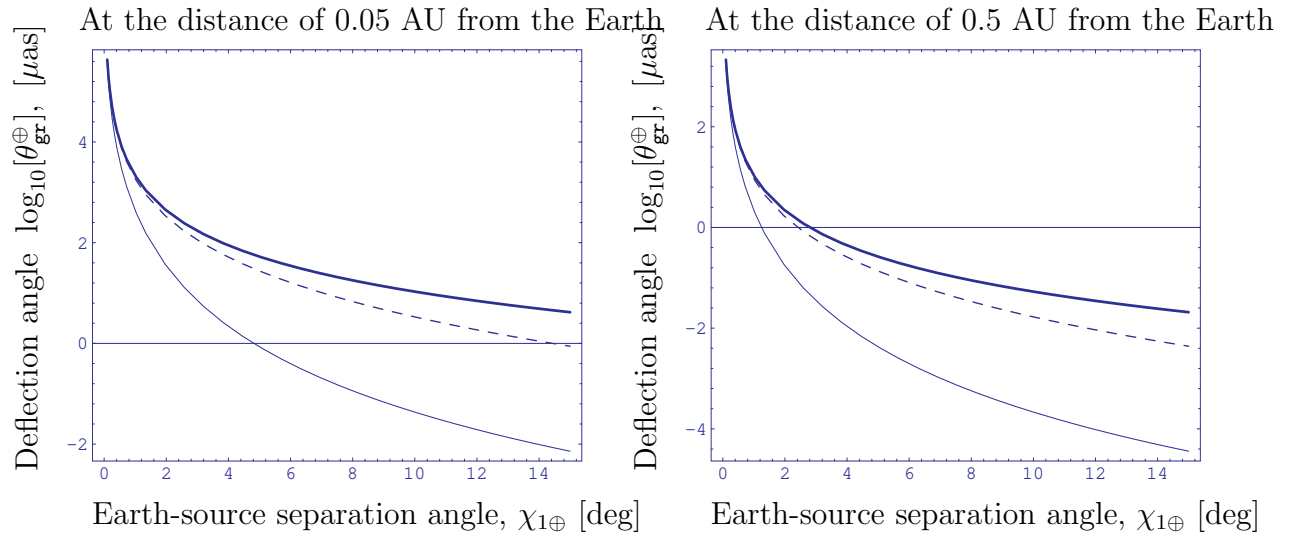


Fig. 5.— Gravitational deflection of light in the proximity of the Earth.

In the Figure 5 we have presented the expected variation in the magnitude of the Earth’s gravity influence as mission progresses. Thus, the left plot is for the end of the first half of the year of the mission, when the spacecraft is at the distance of 0.05 AU from the Earth. The plot on the right side is for the end of the 5-th year of the mission, when SIM is at 0.5 AU from Earth.

## 4. Constraints Derived From the Monopole Deflection of Light

While analyzing the solar gravity field’s influence on the future astrometric observations with SIM, we found several interesting situations, that may potentially put an additional navigational requirements. In this section we will consider these situations in a more detailed way.

### 4.1. Accuracy of Impact Parameter and Planetary Barycentric Position

To carry out an adequate reduction of observations with a  $\Delta\theta_0 = \Delta k \mu\text{as}$  accuracy, it is necessary to determine precisely the value of impact parameter of photon’s trajectory with respect to the body that deflects the photon’s motion from the rectilinear one. As before, we will present two types of necessary expressions, namely for absolute and differential observations. By using the equation (8), one may present the uncertainty  $\Delta d_B$  in determining the impact parameter for a single ray as follows

$$\Delta d_B = \Delta\theta_0 \frac{r_B^2 \sin^2 \chi_{1B}}{2\mu_B} \cdot \frac{\cos \chi_{1B}}{1 + \cos \chi_{1B}}. \quad (24)$$

The corresponding result for differential observations may be obtained with the help of Eq.(12) as:

$$\Delta d_B^{\text{diff}} = \Delta\theta_0 \frac{r_B^2 \sin^2 \chi_{1B}}{4\mu_B} \cdot \left[ 1 + \tan \frac{\chi_{1B}}{2} \cdot \cot \frac{1}{2}(\chi_{2B} - \chi_{1B}) \right]. \quad (25)$$

Similarly, the uncertainty in determining the barycentric distance  $r_B$  should be less then given by the formula below:

$$\Delta r_B = \Delta\theta_0 \frac{r_B^2}{2\mu_B} \cdot \frac{\sin \chi_{1B}}{1 + \cos \chi_{1B}}. \quad (26)$$

A similar expression for the uncertainty in barycentric position  $\Delta r_B^{\text{diff}}$  for differential observations does not produce any constraints significantly different from those derived from Eq.(26), thus we decided not to use it in our analysis. Looking at the results presented in the Table 8, one may see that for astrometric accuracy  $\Delta\theta_0 = 1 \mu\text{as}$  our estimates resulted in fact that one must know the impact parameters with respect to the center of mass of the Sun with the accuracy of  $\sim 0.4 \text{ km}$  (grazing rays), the Jupiter with the accuracy of  $\sim 4 \text{ km}$  and other big planets with the accuracy of about  $10 \text{ km}$ . The corresponding estimates are given in the Table 8. In order to compare these derived requirements on of the barycentric positions of the solar system’s bodies with the current state-of-the-art in their determination, we presented the best known accuracies in the Table 9. The best known accuracies were taken form DE405/LE405.

Table 8: Required accuracy of barycentric positions and impact parameters for astrometric observations with accuracy of  $1 \mu\text{as}$ . The Earth is taken at the distance of 0.05 AU from the spacecraft. Accuracy for the Moon’s position is given from the geocentric reference frame.

Solar system’s object	Required knowledge: grazing rays			Required knowledge: differential astrometry			
	Distance, $\sigma_{r_B}$ , km	Impact parameter		Impact param. [ $15^\circ$ ]		Impact param. [ $1^\circ$ ]	
		$\sigma_{d_B}$ , km	$\sigma_{d_B}$ , mas	$\sigma_{r_B}$ , km	$\sigma_{r_B}$ , mas	$\sigma_{r_B}$ , km	$\sigma_{r_B}$ , mas
Sun	85.45	0.39	0.55	0.40	0.55	0.50	0.69
Sun at $45^\circ$	$1.5 \times 10^4$	$7.6 \times 10^3$	$10''.49$	$3.81 \times 10^4$	$52''.53$	$4.45 \times 10^5$	$613''.66$
Moon	$2.8 \times 10^5$	67.14	$1''.85$	67.17	$1''.85$	68.00	$1''.88$
Mercury	$1.1 \times 10^6$	29.39	66.16	29.41	66.16	29.45	66.25
Venus	$8.4 \times 10^4$	12.18	61.00	12.28	61.20	12.38	62.70
Earth-Moon	$1.3 \times 10^4$	11.14	306.55	11.15	307.47	11.66	321.54
Mars	$6.8 \times 10^5$	29.29	77.11	29.30	77.14	29.37	77.33
Jupiter	$3.8 \times 10^4$	4.31	1.42	4.32	1.42	4.34	1.42
Jupiter at $30''$	$4.9 \times 10^4$	7.14	2.34	7.20	2.36	7.25	2.38
Saturn	$2.2 \times 10^5$	10.32	1.66	10.34	1.66	10.36	1.66
Uranus	$1.2 \times 10^6$	11.27	0.86	11.28	0.86	11.29	0.86
Neptune	$1.7 \times 10^6$	10.04	0.47	10.04	0.47	10.04	0.47
Pluto	$2.0 \times 10^9$	1133.92	40.7	1133.93	40.7	1133.96	40.7

#### 4.1.1. *Need for Improvement of Knowledge of Planetary Positions*

One may see that the present accuracy of knowledge of the inner planets' positions from the Table 9 is given by the radio observations and it is even better than the level of relativity requirements given in the Table 8. However, the positional accuracy for the outer planets is significantly below the required level. The SIM observation program should include the astrometric studies of the outer planets in order to minimize the errors in their positional accuracy determination. Thus, in order to get the radial uncertainty in Pluto's ephemeris with accuracy below 1000 km, it is necessary only 4 measurements of Pluto's position, taken sometime within a week of the stationary points, spread over 3 years. Each measurement could be taken with an accuracy of about 200  $\mu\text{as}$ , as suggested by Standish (1995). Additionally, one will have to significantly lean on the radio observations in order to conduct the reduction of the optical data with an accuracy of a few  $\mu\text{as}$ . For this reason one will have to use the precise catalog of the radio-sources and to study the problem of the radio and optical reference frame ties (Standish (1995); Standish et al (1995); Folkner et al (1994)).

An important way to improve the accuracy of the positions of the outer planets may be offered by the current program of the deep space exploration. Thus, one may expect a factor of 3 improvement in positional accuracy of the Jupiter and its satellites with the completion of the Galileo mission. The Cassini mission will be in the Saturn's vicinity at the time close to the SIM's active astrometric campaign — 2009-2015. A factor of  $3 \times 10^2$  improvement in the Saturn's system positional accuracy may be expected. The Doppler, range and range-rate measurements to the spacecraft, combined together with the ground-based VLBI methods will significantly improve the positional accuracy for the bodies in the solar system. This will help to increase the overall accuracy of the SIM astrometric observations via a frame tie to the radio and the dynamical reference frames.

From the other hand, the accuracy of a single measurement with SIM is expected to be of the order of  $\sigma_\alpha = 8 \mu\text{as}$ . If the uncertainty in positions may contribute only to about 10% of the total variance, thus  $\Delta\theta_0 = \sqrt{0.1}\sigma_\alpha = 2.53 \mu\text{as}$ . This fact relaxes requirements presented in the Table 8. However, even though the requirements are still much smaller the current best knowledge, it may be the case when SIM actually will significantly improve positions of outer planets of the solar system simply as a by-product of it's astrometric campaign. To correctly address this problem one needs to perform a full-blown numerical simulation with a complete model for the SIM instrument.

Table 9: The best known accuracies of barycentric positions and masses for the solar system’s objects derived from DE405/LE405. Planetary masses taken from Yoder (1995).

Solar system’s object	Knowledge of barycentric position		Method used for determination	Knowledge of planetary masses, $\Delta M_B/M_B$
	Best known,			
	$\sigma_{r_B}$ , km	$\sigma_{r_B}$ , mas		
Sun	362/725	0".5/1".0	Optical meridian transits	$3.77 \times 10^{-10}$
Moon	27 cm	7.4 $\mu$ as	LLR, 1995	$1.02 \times 10^{-6}$
Mercury	1	2.25	Radar ranging	$4.13 \times 10^{-5}$
Venus	1	4.98	Radar ranging	$1.23 \times 10^{-7}$
Earth	1	27.58	Radar ranging	TBD $\times 10^{-6}$
Mars	1	2.63	Radar ranging	$2.33 \times 10^{-6}$
Jupiter	30	9.84	Radar ranging	$7.89 \times 10^{-7}$
Saturn	350	56.24	Optical astrometry	$2.64 \times 10^{-6}$
Uranus	750	57.00	Optical astrometry	$3.97 \times 10^{-6}$
Neptune	3,000	141.67	Optical astrometry	$2.19 \times 10^{-6}$
Pluto/Charon	20,000	717.40	Photographic astrometry	0.014

Table 10: Required accuracy of the planetary masses, the PPN parameter  $\gamma$  and the uncertainty in the attitude determination for the astrometric error allocation of 1  $\mu$ as.

Solar system’s object	Masses, $\Delta M_B/M_B$	PPN parameter $\gamma$		Attitude accuracy [15°], $\Delta(\epsilon - \alpha_B)$
		$\Delta\gamma$	$\Delta\gamma_{\text{diff}}$ [15°]	
Sun	$5.7 \times 10^{-7}$	$1.1 \times 10^{-6}$	$1.2 \times 10^{-6}$	0".124
Sun at 45°	$1.0 \times 10^{-4}$	$2.0 \times 10^{-4}$	$7.1 \times 10^{-4}$	73".23
Moon	$3.8 \times 10^{-2}$	$7.7 \times 10^{-2}$	$7.7 \times 10^{-2}$	2°.21
Mercury	$1.2 \times 10^{-2}$	$2.4 \times 10^{-2}$	$2.4 \times 10^{-2}$	0°.69
Venus	$2.0 \times 10^{-3}$	$4.1 \times 10^{-3}$	$4.1 \times 10^{-3}$	0°.12
Earth	$1.7 \times 10^{-3}$	$3.4 \times 10^{-3}$	$3.5 \times 10^{-3}$	361".00
Mars	$8.6 \times 10^{-3}$	$1.7 \times 10^{-2}$	$1.7 \times 10^{-2}$	0°.49
Jupiter	$6.1 \times 10^{-5}$	$1.2 \times 10^{-4}$	$1.2 \times 10^{-4}$	12".38
Jupiter at 30"	$7.9 \times 10^{-5}$	$1.5 \times 10^{-4}$	$1.6 \times 10^{-4}$	16".50
Saturn	$1.7 \times 10^{-4}$	$3.4 \times 10^{-4}$	$3.4 \times 10^{-4}$	35".07
Uranus	$4.6 \times 10^{-4}$	$9.2 \times 10^{-4}$	$9.2 \times 10^{-4}$	94".88
Neptune	$3.9 \times 10^{-4}$	$7.9 \times 10^{-4}$	$8.0 \times 10^{-4}$	82".51
Pluto	0.35	0.71	0.71	20°.34

## 4.2. Accuracy of Planetary Masses and the PPN Parameter $\gamma$

The uncertainty in determining the solar and the planetary masses  $\Delta M_B$  should be less than given by the formula below:

$$\frac{\Delta M_B}{M_B} = \Delta\theta_0 \frac{r_B}{2\mu_B} \cdot \frac{\sin \chi_{1B}}{1 + \cos \chi_{1B}}. \quad (27)$$

The corresponding estimates for  $\Delta\theta_0 = 1 \mu\text{as}$  are presented in the Table 10. Thus, the presently available values for the planetary masses, given in Table 9, are more than sufficient to fulfill the general relativistic requirements.

Similarly, the uncertainty in determining the PPN parameter  $\gamma$  should be less than given by the following expression:

$$\Delta\gamma = \Delta\theta_0 \frac{r_B}{\mu_B} \cdot \frac{\sin \chi_{1B}}{1 + \cos \chi_{1B}}. \quad (28)$$

Finally, the relation for the differential astrometric measurements one obtains in the form:

$$\Delta\gamma_{\text{diff}} = \Delta\theta_0 \frac{r_B}{\mu_B} \cdot \frac{\sin \frac{1}{2}\chi_{1B} \sin \frac{1}{2}\chi_{2B}}{\sin \frac{1}{2}(\chi_{2B} - \chi_{1B})}. \quad (29)$$

The corresponding results for uncertainties in the planetary masses and PPN parameters  $\gamma$  needed for  $\Delta\theta_0 = 1 \mu\text{as}$  astrometric accuracy are given in the Table 10. Presently the best known determination of the PPN parameter  $\gamma$  is  $|\gamma - 1| \leq 3 \times 10^{-4}$  and was given by Eubanks et al (1997). [Note that the authors have made a very first attempt to include the post-PN effects (e.g  $\propto G^2$ ) into their model and corresponding VLBI data analysis.] Thus, the value of this PPN parameter will have to be improved either before SIM will be launched or by the mission itself.

## 4.3. Astrometric Test of General Relativity

### 4.3.1. Solar Gravity Field as a Deflector

To model the astrometric data to the nominal measurement accuracy will require including the effect of general relativity on the propagation of light. In the PPN framework, the parameter  $\gamma$  would be part of this model and could be estimated in global solutions. The astrometric residuals may be tested for any discrepancies with the prescriptions of general relativity. To address this problem in a more detailed way, one will have to use the astrometric model for the instrument including the information about its position in the solar



system, it's attitude orientation in the proper reference frame, the time history of different pointings and their durations, etc. This information then should be folded into the parameter estimation program that will use a model based on the expression, similar to that given by Eq.(10). In addition, due to the geometric constraints of the spacecraft's orbit in the solar system, one may expect that solution for the parameter  $\gamma$  will be highly correlated with the solution for parallaxes.

Taking into account the fact that presently we are lacking the existence of a real data, we may only estimate a possibility of increasing the accuracy of the parameter's  $\gamma$  determination. Thus, the estimates from the Table 1 have demonstrated that effect of gravitational deflection of light may be used to estimate the value of PPN parameter  $\gamma$  at a scientifically important level. Most important is that the corresponding result could be obtained simply as a by-product of the SIM astrometric campaign (see Turyshev (1998)). For the crude estimation purposes one may present the expected accuracy of the parameter  $\gamma$  determination in a single astrometric measurement as:

$$\Delta\gamma = \Delta\theta_0 \frac{r_{\odot}^{\text{SIM}}}{\mu_{\odot}} \frac{\sin \frac{1}{2}\chi_{1\odot} \sin \frac{1}{2}\chi_{2\odot}}{\sin \frac{1}{2}(\chi_{2\odot} - \chi_{1\odot})}, \quad (30)$$

where  $\Delta\theta_0$  is the largest tolerable error in the total error budget allowed for the stellar aberration due to relativistic deflection of light in the solar system.

The relativity test will be enhanced by scheduling measurements of stars as close to the Sun as possible. Despite the fact that during it's observing campaign, SIM will never be closer to the Sun than  $45^\circ$ , it is still will allow for an accurate determination of this PPN parameter. Thus, a single astrometric measurement with SIM is expected to be with an accuracy of  $\sigma_{\alpha} = 8 \mu\text{as}$ . It seems to be a reasonable assumption that a contribution of any component of the total error budget should not exceed 10% of the total variance a single accuracy of  $\sigma_{\alpha}^2$ . This allows to estimate the correction factor  $\Delta\theta_0$  in Eq.(30) to be  $\Delta\theta_0 = 8\sqrt{0.1} = 2.52982 \mu\text{as}$ . Thus, at the rim of the solar avoidance angle,  $\chi_{1\odot} = 45^\circ$ , one could determine this parameter with an accuracy  $|\gamma - 1| \sim 1.79 \times 10^{-3}$  in a single measurement. When the mission progresses the accuracy of this experiment will improve as  $1/\sqrt{N}$ , where  $N$  is the number of independent observations. With  $N \sim 5000$ , SIM may achieve accuracy of  $\sigma_{\gamma} \sim 2.4 \times 10^{-5}$  in astrometric tests of general relativity in the solar gravity field.

#### 4.3.2. GR Test in the Jovian and Earth' Gravity Fields

It is worth noting that one could perform relativity experiment not only with the Sun, but also with the Jupiter and the Earth. In fact, for the proposed SIM's observing mode, the

accuracy of determining of the parameter  $\gamma$  may be even better than that achievable with the Sun. Indeed, with the same assumptions as above, one may achieve a single measurement the accuracy of  $|\gamma - 1| \sim 4.0 \times 10^{-4}$  determined via deflection of light by Jupiter. However, astrometric observations in the Jupiter’s vicinity are the targeted observations. One will have to specifically plan those experiments in advance. This fact is minimizing the number of possible independent observations and, as a result, the PPN parameter  $\gamma$  may be obtained with accuracy of about  $\sigma_\gamma \sim 1.3 \times 10^{-5}$  with astrometric experiments in the Jupiter’s gravity field (note that only  $N \sim 1000$  needed). For a long observing times  $\sim 10^3$  sec the Jupiter’s orbital motion could significantly contribute to this experiment (see Sec.4.5 for details).

Lastly, let us mention that the experiments conducted in the Earth’s gravity field, could also determine this parameter to an accuracy  $|\gamma - 1| \sim 8.9 \times 10^{-3}$  in a single measurement (which in return extends the measurement of the gravitational bending of light to a different mass and distances scale, as shown by Gould (1993)). One may expect a large statistics gained from both the astrometric observations and the telecommunications with the spacecraft. This, in return, will significantly enhance the overall solution for  $\gamma$  obtained in the Earth’ gravitational environment.

#### 4.4. Baseline Orientation and the Attitude Control Accuracy

At this point we would like to study the effect of the attitude determination uncertainty on the accuracy of the astrometric data correction for the effect of gravitational deflection of light. In order to estimate the tolerable uncertainty in determining the orientation of the baseline vector  $\vec{b}$  and the vector of spacecraft’s position with respect to the deflector,  $\alpha_B$ , we will use the equation Eq.(10). With the help of this equation one obtains the following expression:

$$\Delta(\epsilon - \alpha_B) = \frac{\Delta\theta_0}{\cos(\epsilon - \alpha_B)} \frac{r_B}{2\mu_B} \frac{\sin \frac{1}{2}\chi_{1B} \sin \frac{1}{2}\chi_{2B}}{\sin \frac{1}{2}(\chi_{2B} - \chi_{1B})}. \quad (31)$$

Thus, the case with  $|\cos(\epsilon - \alpha_B)| = 1$  is the most accuracy demanding orientation of the vectors involved. Corresponding estimates for  $\Delta\theta_0 = 1 \mu\text{as}$  are presented in the Table 10. Deflection of light by the Jupiter puts the most stringent requirement on the attitude control and baseline orientation of  $\Delta\epsilon \approx \Delta\alpha_B = 16''.50/\sqrt{2} = 11''.67$ . However, in accord to the current error budget allocations, which is bookkeeping a much smaller number (e.g.  $\sim$  few mas), this requirement will be easily met.

#### 4.5. Stellar Aberration Introduced by the Orbital Motion of a Deflector

The orbital motion of the deflecting bodies could significantly contribute to the relativistic deflection measurement. To estimate this influence, let us assume that during the experiment the deflecting body moves with velocity  $\vec{v}_B$ . This motion will result in the time-dependent change of the impact parameter  $d_B$ . Such a variation could produce an additional angular drift with the rate  $\dot{\theta}_{\text{gr}}^B$ , in addition to the static monopole deflection Eq.(8). For the estimation purposes, it is convenient to express the total effect of the monopole deflection Eq.(8) and this aberrational correction in terms of the deflector-source sky separation angle  $\chi_{B_0}$  at the beginning of the experiment.

Thus, a circular orbital motion of the deflecting body produces a drift in the deflector-source separation angle on the sky,  $\chi_B(t)$ , given by the expression

$$\chi_B(t) = \chi_B(t_0) + \dot{\chi}_{B_0} \cdot (t - t_0) + \mathcal{O}(t^2), \quad (32)$$

where  $\chi_B(t_0) = \chi_{B_0}$  is the initial observing angle, and  $\dot{\chi}_{B_0} = v_B/r_B$  is the rate of corresponding angular drift. Assuming that  $\dot{\chi}_{B_0}$  is small and for short time spans  $\Delta t$ , one may expand the quantities in the terms of the small parameter  $(v_B \Delta t)/(r_B \chi_{B_0})$ . [This is done for estimation purposes only. In a real situation there may not be a small parameter at all. In this case a full-blown numerical integration should be used instead.]

##### 4.5.1. Rate of Absolute Drift Due to Planetary Motion

As a result of a simplification discussed above, the total time-dependent effect of the gravitational deflection of light may be presented by the expression (similar to the concept of a retarget action):

$$\theta_{\text{gr}}^B(t) = \theta_{\text{gr}}^B(t_0) - \dot{\theta}_{\text{gr}}^B \cdot (t - t_0) + \mathcal{O}(\Delta t^2), \quad (33)$$

where the first term is the static gravitational deflection angle at the beginning of the experiment:

$$\theta_{\text{gr}}^B(t_0) = (\gamma + 1) \frac{\mu_B}{r_B} \frac{1 + \cos \chi_{B_0}}{\sin \chi_{B_0}} \quad (34)$$

with the values for the solar system bodies (for grazing rays!, e.g.  $r_B \sin \chi_{B_0} = d_B = \mathcal{R}_B$ ) given in the Table 1. The second term on the right-hand side of Eq.(32) is the rate of the angular drift due to the planetary motion. This quantity may be presented in the following

form:

$$\dot{\theta}_{\text{gr}}^B = \frac{\mu_B v_B}{r_B^2 \sin^2 \frac{1}{2} \chi_{B_0}}. \quad (35)$$

Magnitudes of the angular drifts  $\dot{\theta}_{\text{gr}}^B$  introduced by the orbital motion of the solar system bodies are given in the Table 11.

#### 4.5.2. Rate of Differential Drift Introduced by Planetary Motion

The expressions for the case of differential observations may be obtained with the help of Eq.(12). We will use the same assumptions on the smallness of the quantities involved as were used above for the case of absolute astrometry. As a result, a linear drift in the planetary position, Eq.(32), introduces a time-variation in the gravitational light bending effect,  $\delta\theta_{\text{gr}}^B(t)$ , as given by the expressions below:

$$\delta\theta_{\text{gr}}^B(t) = \delta\theta_{\text{gr}}^B(t_0) - \delta\dot{\theta}_{\text{gr}}^B \cdot (t - t_0) + \dot{\lambda}_{\text{SIM}}^B \cdot (t - t_0) + \mathcal{O}(\Delta t^2), \quad (36)$$

where the first term is the static differential deflection angle at the beginning of observations

$$\delta\theta_{\text{gr}}^B(t_0) = (\gamma + 1) \frac{\mu_B}{r_B} \frac{\sin \frac{1}{2}(\chi_{2B_0} - \chi_{1B_0})}{\sin \frac{1}{2}\chi_{1B_0} \cdot \sin \frac{1}{2}\chi_{2B_0}} \quad (37)$$

with the values for the solar system bodies presented in the Table 1. The second term on the right-hand side of Eq.(36) is the rate of the differential angular drift due to the planetary motion. This quantity is given as follows:

$$\delta\dot{\theta}_{\text{gr}}^B = \frac{\mu_B v_B}{r_B^2} \left[ \frac{1}{\sin^2 \frac{1}{2}\chi_{1B_0}} - \frac{1}{\sin^2 \frac{1}{2}\chi_{2B_0}} \right]. \quad (38)$$

The last term in the Eq.(36),  $\dot{\lambda}_{\text{SIM}}^B$ , is introduced by any temporal drifts in the accuracy of the SIM instrument during observations:

$$\dot{\lambda}_{\text{SIM}}^B = \frac{\mu_B}{r_B} \frac{\Delta\dot{\chi}_0}{\sin^2 \frac{1}{2}\chi_{2B_0}} = \frac{\mu_B}{r_B} \frac{\Delta\dot{\chi}_0}{\sin^2 \frac{1}{2}(\chi_{1B_0} + \Delta\chi_0)}, \quad (39)$$

where  $\Delta\chi_0 = \chi_{2B_0} - \chi_{1B_0}$  is the angular separation between the two sources at the beginning of the observation and  $\Delta\dot{\chi}_0 = \dot{\chi}_{2B_0} - \dot{\chi}_{1B_0}$  is any time drift in estimating this separation introduced by the instrument [e.g. temporal drifts inside the observed tile due to possible time-varying drifts in the instrument's metrology]. However, it turns out that this effect is

Table 11: Relativistic planetary aberration of light due to their barycentric orbital motion. For the purposes of this study, we assumed SIM at a fixed position in the solar system with  $v_{\text{SIM}} = 0$ . Aberration due to the solar system’s galactocentric motion is unobservable.

Solar system’s object	Velocity, km/sec	$\dot{\theta}_{\text{gr}}^B$ , $\mu\text{as/s}$	$\delta\dot{\theta}_{\text{gr}}^B [15^\circ]$ , $\mu\text{as/s}$	$\delta\dot{\theta}_{\text{gr}}^B [1^\circ]$ , $\mu\text{as/s}$
Sun (galactic)	220	553.5	553.2	558.9
Sun	0.013	0.033	0.033	0.031
Sun at $45^\circ$	-same-	$4 \times 10^{-7}$	$5 \times 10^{-7}$	$5 \times 10^{-8}$
Moon	0.04	$6 \times 10^{-4}$	$6 \times 10^{-4}$	$6 \times 10^{-4}$
Mercury	47.87	1.63	1.63	1.63
Venus	35.05	2.86	2.86	2.86
Earth	29.80	2.68	2.71	2.71
Mars	24.14	0.82	0.82	0.82
Jupiter	13.1	3.04	3.04	3.04
Jupiter at $30''$	-same-	1.82	1.82	1.82
Saturn	9.63	0.93	0.93	0.93
Uranus	6.81	0.60	0.60	0.60
Neptune	5.44	0.54	0.54	0.54
Pluto	4.75	$4 \times 10^{-3}$	$4 \times 10^{-3}$	$4 \times 10^{-3}$

not important for our study. Indeed, even for the most intense gravitational environment, at the solar avoidance angle with  $\chi_{1B_0} = 45^\circ$ , and for the maximal star separation  $\Delta\chi_0 = 15^\circ$ , a constant linear drift with the rate of  $\Delta\dot{\chi}_0 = 50 \text{ mas/s}$ , produces a total effect of only  $\dot{\lambda}_{\text{SIM}}^B = 0.002 \text{ } \mu\text{as/sec}$ .

The quantities characterizing the dynamical astrometric environment in the vicinity of the solar system’s bodies are presented in the Table 11. Due to the fact that the differential effect behaves as  $\sim [1/\sin^2(\text{small\_angle}) - 1/\sin^2(\text{small\_angle} + \text{FoR}/2)]$  it is almost insensitive to the sizes of the two available fields of regard. Thus, independently on the size of the available field of regard, the consideration of the orbital velocity of planet’s motion turns out to be a significant issue, especially for the Jupiter and some inner planets. One will have to account for this effect during a long exposure observations, say for  $t \sim 10^3 \text{ sec}$ .

Concluding, let us mention that the presented estimates were given for the static gravitational field in the barycentric RF. Analysis of a real experimental situation should consider a non-static gravitational environment of the solar system and should include the descrip-

tion of light propagation in a different RFs involved in the experiment. Additionally, the observations will be affected by the relativistic orbital dynamics of the spacecraft.

#### 4.6. Solar Acceleration Towards the Galactic Center

The Sun’s absolute velocity with respect to a cosmological reference frame was measured photometrically: it shown up as the dipole anisotropy of the cosmic microwave background. The Sun’s absolute acceleration with respect to a cosmological reference frame can be measured astrometrically: it will show up as proper motion of quasars.

The aberration due to the solar system’s galactocentric motion will not be observable. However, the rate of this aberration will produce an apparent proper motion for the observed sources. Indeed, the solar system’s orbital velocity around the galactic center causes an aberrational affect of the order of 2.5 arcmin. All measured star and quasar positions are shifted towards the point on the sky having galactic coordinates  $l = 90^\circ$ ,  $b = 0^\circ$ . For an arbitrary point on the sky the size of the effect is  $2.5 \sin \eta$  arcmin, where  $\eta$  is the angular distance to the point  $l = 90^\circ$ ,  $b = 0^\circ$ . The acceleration of the solar system towards the galactic center causes this aberrational effect to change slowly. This leads to a slow change of the apparent position of distant celestial objects, i.e. to an apparent proper motion.

Let us assume a solar velocity of 220 km/sec and a distance of 8.5 kpc to the galactic center. The orbital period of the Sun is then 250 million years, and the galactocentric acceleration takes a value of about  $1.75 \times 10^{-13}$  km/sec<sup>2</sup>. Expressed in a more useful units it is 5.5 mm/s/yr. A change in velocity by 5.5 mm/sec causes a change in aberration of the order of 4  $\mu$ as. The apparent proper motion of a celestial object caused by this effect always points towards the direction of the galactic center. Its size is  $4 \sin \eta$   $\mu$ as/yr, where  $\eta$  is now the angular distance between the object and the galactic center.

The above hold in principle for quasars, for which it can be assumed that the intrinsic proper motions (i.e. those caused by real transverse motions) are negligible. A proper motion of 4  $\mu$ as/yr corresponds to a transverse velocity of  $2 \times 10^4$  km/sec at  $z = 0.3$  for  $H_0=100$  km/sec/Mpc, and to  $4 \times 10^4$  km/sec for  $H_0 = 50$  km/sec/Mpc. Thus, all quasars will exhibit a distance-independent steering motion towards the galactic center. Within the Galaxy, on the other hand, the effect is drowned in the local kinematics: at 10 pc it corresponds to only 200 m/sec.

However, for a differential astrometry with SIM this effect will have to be scaled down to account for the size of the field of regard Turyshev & Unwin (1998), namely  $2 \sin \frac{\text{FoR}}{2} = 2 \sin \frac{\pi}{24} = 0.261$ . This fact is reducing the total effect of the galactocentric acceleration to

only  $\sim 1 \sin \eta \mu\text{as/yr}$  and, thus, it makes the detection of the solar system’s galactocentric acceleration with SIM to be a quite problematic issue.

## 5. Deflection of Light by the Higher Multipoles of the Gravity Field

In order to carry out a complete analysis of the phenomenon of the relativistic light deflection one should account for other possible terms in the expansion (1) that may potentially contribute to this effect. These terms are due to non-sphericity and non-staticity of the body’s gravity field.

### 5.1. Gravitational Quadrupole Deflection of Light

Effect of the gravitational deflection of light caused by the quadrupole term may be given as Turyshev (1998):

$$\theta_{J_2} = \frac{1}{2}(\gamma + 1) \frac{4GM}{c^2 \mathcal{R}} J_2 (1 - s_z^2 - 2d_z^2) \left(\frac{\mathcal{R}}{d}\right)^3, \quad (40)$$

where  $J_2$  is the second zonal harmonic of the body under question,  $\vec{s} = (s_x, s_y, s_z)$  is the unit vector in the direction of the light ray propagation and vector  $\vec{d} = d(d_x, d_y, d_z)$  is the impact parameter. A similar expression may be obtained for the differential observations. This formula, for estimation purposes only, may be given as follows:

$$\delta\theta_{J_2} \approx \frac{4\mu_B J_{2B} \mathcal{R}_B^2}{r_B^3} \left[ \frac{1}{\sin^3 \chi_{1B}} - \frac{1}{\sin^3 \chi_{2B}} \right]. \quad (41)$$

The corresponding effects for the deflection of light by the quadrupole mass distribution in the solar system planets are given in the Table 13. Note that the effect of the quadrupole deflection of light depends on a number of different instantaneous geometric parameters defining the mutual orientation of the vector of the light propagation, position of the planet in orbit, the orientation of the axes defining it’s figure, etc. This to model this effect will require a significant effort.

This effect depends on the third power of the inverse impact parameter. This fact together with a small planetary angular sizes (compare to the size of the SIM’s field of regard) makes it insensitive to the size of the FoR for differential astrometry. Note that the measurements of the quadrupole deflection have never been done before. SIM will allow to measure this effect directly for the first time. At the expected level of accuracy the knowledge of some fundamental phenomena, such as the jovian atmosphere, the magnetic

Table 12: Higher gravitational coefficients for solar system bodies. The data taken from <http://nssdc.gsfc.nasa.gov/planetary/factsheet/>

Solar system's object	$J_2^B,$ $\times 10^{-6}$	$J_4^B,$ $\times 10^{-6}$	$J_6^B,$ $\times 10^{-6}$
Sun	$0.17 \pm 0.017$	—	—
Sun at 45°	—	—	—
Moon	202.2	-0.1	—
Mercury	60.	—	—
Venus	4.5	-2.1	—
Earth	1,082.6	-1.6	0.5
Mars	1,960.45	—	—
Jupiter	$14,738 \pm 1$	$-587 \pm 5$	$34 \pm 50$
Saturn	$16,298 \pm 50$	$-915 \pm 80$	103.0
Uranus	3,343.43	—	—
Neptune	3,411.	—	—
Pluto	—	—	—

field fluctuations, etc., may contribute to the errors in the experiment Treuhaft & Lowe (1991).

As a result, one will have to account for the quadrupole component of the gravity fields of the outer planets. In addition, the influence of the higher harmonic may be also of interest. Let us estimate the influence of some gravitational multipole moments of Jupiter and Saturn, which are presented in the Table 13. It is convenient to discuss the deflection by the  $J_2$  and  $J_4$  coefficients of the jovian gravity in terms of the Jupiter-source separation angle  $\chi_{1J}$ . An expression, similar to that of Eq.(20) for the monopole deflection, may be obtained for the jovian quadrupole deflection in terms of the Jupiter-source separation angle  $\chi_{1S}$ . The quadrupole deflection angle in this case may be given as:

$$\theta_{J_2}^{\max} = 3.46058 \times 10^{-10} \frac{1}{\sin^3 \chi_{1J}} \mu\text{as}. \quad (42)$$

The Jupiter's angular dimensions from the Earth are calculated to be  $\mathcal{R}_J = 23.24$  arcsec, which correspond to a deflection angle of 242  $\mu\text{as}$ . The deflection on the multipoles for some  $\chi_{1J}$  is given in the Table 14.

A similar studies could be performed for the Saturn. In terms of the Saturn-source separation angle  $\chi_{1S}$  the saturnian quadrupole deflection mat be estimated with the help of



Table 13: Relativistic quadrupoles deflection of light by the bodies in the solar system.

Solar system' object	$J_2^B,$ $\times 10^{-6}$	$\theta_{J_2}^B,$ $\mu\text{as}$	$d_{J_2}^{\text{crit}}$	$\delta\theta_{J_2}^B[15^\circ],$ $\mu\text{as}$	$\delta\theta_{J_2}^B[1^\circ],$ $\mu\text{as}$
Sun	$0.17 \pm 0.017$	0.3	—	0.3	0.3
Moon	202.2	$2 \times 10^{-2}$	—	$2 \times 10^{-2}$	$2 \times 10^{-2}$
Mercury	60.	$5 \times 10^{-3}$	—	—	—
Venus	4.5	$2 \times 10^{-3}$	—	—	—
Earth	1,082.6	0.6	—	0.6	0.6
Mars	1,960.45	0.2	—	0.2	0.2
Jupiter	$14,738 \pm 1$	242.0	$98''.12 - 144''.81$ $6.23 \mathcal{R}_J$	242.0	242.0
Saturn	$16,298 \pm 50$	94.6	$35''.62 - 43''.93$ $4.56 \mathcal{R}_S$	94.6	94.6
Uranus	3,343.43	7.3	$3''.25 - 3''.61$ $1.94 \mathcal{R}_U$	7.3	7.3
Neptune	3,411.	8.5	$2''.23 - 2''.42$ $2.04 \mathcal{R}_N$	8.5	8.5
Pluto	—	—	—	—	—

the following expression:

$$\theta_{J_2}^{\text{max}} = 9.66338 \times 10^{-12} \frac{1}{\sin^3 \chi_{1S}} \mu\text{as}. \quad (43)$$

The Saturn's angular dimensions from the Earth' orbit are calculated to be  $\mathcal{R}_S = 9.64$  arcsec, which correspond to a deflection angle of  $94.7 \mu\text{as}$ . The corresponding estimates for the deflection angles are presented in the Table 15.

As a result, for astronomical observations with accuracy of about  $1 \mu\text{as}$ , one will have to account for the quadrupole gravitational fields of the Sun, Jupiter, Saturn, Neptune, and Uranus. In addition, the influence of the higher harmonics may be of interest. For example some of the moments for Jupiter and Saturn are given in the Table 12. Concluding this paragraph, we would like to note that the higher multipoles may also influence the astrometric observations taken close to these planets. Thus, for both Jupiter and Saturn the rays, grazing their surface, will be deflected by the fourth zonal harmonic  $J_4$  as follows:  $\delta\theta_{J_4}^J \approx 9.6 \mu\text{as}$ ,  $\delta\theta_{J_4}^S \approx 5.3 \mu\text{as}$ . In addition, the contribution of the  $J_6$  for Jupiter and Saturn will deflect the grazing rays on the angles  $\delta\theta_{J_6}^J \approx 0.8 \mu\text{as}$ ,  $\delta\theta_{J_6}^S \approx 0.6 \mu\text{as}$ . The contribution of  $J_4$  is decreasing with the distance from the body as  $d^{-5}$  and contribution of  $J_6$  as  $d^{-7}$ . As

Table 14: Deflection of light by the Jovian higher gravitational coefficients.

Jovian deflection	$\chi_{1J}$ , arcsec						
	23".24	26"	30"	35"	40"	50"	120"
$\theta_{J_2}^J$ , $\mu\text{as}$	242	173	112	71	47	24	1.8
$\delta\theta_{J_2}^J[15^\circ]$ , $\mu\text{as}$	242	173	112	71	47	24	1.8
$\theta_{J_4}^J$ , $\mu\text{as}$	9.6	5.5	2.7	1.3	0.6	0.2	0.0

Table 15: Deflection of light by the Saturnian higher gravitational coefficients.

Saturnian deflection	$\chi_{1S}$ , arcsec						
	9".64	12"	15"	20"	25"	30"	35"
$\theta_{J_2}^S$ , $\mu\text{as}$	94.7	49.1	25.1	10.6	5.4	3.1	2
$\delta\theta_{J_2}^S[15^\circ]$ , $\mu\text{as}$	94.7	49.1	25.1	10.6	5.4	3.1	2
$\theta_{J_4}^S$ , $\mu\text{as}$	5.3	1.8	0.6	0.1	—	—	—

a result the deflection angle will be less than  $1 \mu\text{as}$  when  $d > 1.6 \mathcal{R}$ , where  $\mathcal{R}$  is the radius of the planet.

### 5.1.1. Critical Distances for Quadrupole Deflection of Light

The critical distance  $d_{J_2}^{\text{crit}}$  for the astrometric observations in the regime of quadrupole deflection of light with accuracy of  $\Delta\theta_0 = \Delta k \mu\text{as}$  was defined as:

$$d_{J_2}^{\text{crit}} = \mathcal{R}_B \left[ \frac{4\mu_B J_2^B}{\mathcal{R}_B \Delta\theta_0} \right]^{\frac{1}{3}}. \quad (44)$$

The critical distances for the relativistic quadrupole deflection of light by the solar system's bodies for the case of  $\Delta k = 1$  presented in the Table 13.

## 5.2. Gravito-Magnetic Deflection of Light

Besides the gravitational deflection of light by the monopole and the quadrupole components of the static gravity field of the bodies, the light ray trajectories will also be affected by the non-static contributions from this field. It is easy to demonstrate that a rotational

motion of a gravitating body contributes to the total curvature of the space-time generated by this same body. This contribution produces an additional deflection of light rays on the angle

$$\delta\theta_{\vec{S}} = \frac{1}{2}(\gamma + 1) \frac{4G}{c^3 d^3} \vec{S}(\vec{s} \cdot \vec{d}), \quad (45)$$

where  $\vec{S}$  is the body's angular momentum.

The most significant contributions of rotation of the solar system bodies to the relativistic light deflection are the following ones: the solar deflection amounts to  $\delta\theta_{\vec{S}}^{\odot} = \pm(0.7 - 1.3)\mu\text{as}$  [the first term listed is for a uniformly rotating Sun; the second is for the Dicke's model]; jovian is about  $\delta\theta_{\vec{S}}^J = \pm 0.2 \mu\text{as}$ ; and saturnian  $\delta\theta_{\vec{S}}^{Sa} = \pm 0.04 \mu\text{as}$ . Thus, depending on the model for the solar interior, solar rotation may produce a noticeable contribution for the grazing rays. The estimates of magnitude of deflection of light ray's trajectory, caused by the rotation of gravitating bodies demonstrate that for precision of observations of  $1 \mu\text{as}$  it is sufficient to account for influence of the Sun and Jupiter only.

The relativistic gravito-magnetic deflection of light has never been tested before. Due to the fact that the magnitudes of corresponding effects in the solar system are too small and, moreover, the SIM operational mode limits the viewing angle for a sources as  $\chi_{1\odot} \geq 45^\circ$ , SIM will not be sensitive to this effect.

## Discussion

General relativistic deflection of light produces a significant contribution to the future astrometric observations with accuracy of about a few  $\mu\text{as}$ . In this Memo we addressed the problem of light propagation on the gravitational field of the solar system. It was shown that for high accuracy observations it is necessary to correct for the post-Newtonian deflection of light by the monopole components of gravitational fields of a large number of celestial bodies in the solar system, namely the Sun and the nine planets, together with the planetary satellites and the largest asteroids (important only if observations are conducted in their close proximity). The most important fact is that the gravitational presence of the Sun, the Jupiter and the Earth should be always taken into account, independently on the positions of these bodies relative to the interferometer. It is worth noting that the post-post Newtonian effects due to the solar gravity will not be accessible with SIM. This effect as well as the effect of gravitational deflection of light caused by the mass quadrupole term of the Sun are negligible at the level of expected accuracy. However, deflection of light by some planetary quadrupoles may have a big impact on the astrometric accuracy. Thus, the higher

gravitational multipoles should be taken into account when observations are conducted in the close proximity of two bodies of the solar system, notably the Jupiter and the Saturn.

We addressed the problem of adequacy of the current level of accuracy of the solar system ephemerides. It turns out that, even though the accuracy in determining the outer planets positions is below the general relativistic requirements, one may expect that SIM will actually improve the planetary ephemerides simply as a by-product of its future astrometric campaign.

As an important result of it's astrometric campaign, SIM could provide an accurate measurement of the PPN parameter  $\gamma$ . Thus, for observations on the rim of the solar avoidance angle one could determine  $\gamma$  to an accuracy of about two parts in  $10^3$  in a single measurement. For a large number of observing pairs of stars such an experiment could potentially determine  $\gamma$  with an accuracy of about  $\sim 10^{-5}$  which is an order of magnitude better than presently known. One could perform experiments with a comparable accuracy in the Jupiter's gravity field. To correctly address this problem an extensive covariance studies are needed.

The reported research has been done at the Jet Propulsion Laboratory, California Institute of Technology, which is under contract to the National Aeronautic and Space Administration.

## REFERENCES

- Perryman, M. A. C., et al. 1992, *A&A*, 258, 1
- Gould, A. 1993, *ApJ*, 414, L37
- Turyshev, S. G. and Unwin, S. C. 1998, *Relativistic Stellar Aberration Requirements for the Space Interferometry Mission*, JPL Technical Memorandum #98-1017, Pasadena, CA.
- Sovers, O. J., Jacobs, C. S. 1996, in *Observation Model and Parameter Partial for the JPL VLBI Parameter Estimation Software "MODEST" - 1996*, JPL Technical Report 83-39, Rev. 6, Pasadena, CA.
- Will, C. M. 1993, *Theory and Experiment in Gravitational Physics*, (Rev. Ed.), Cambridge Univ. Press, Cambridge, England.
- Dar, A. 1992, *Nucl. Phys.*, **B** (Suppl.), 28A, 321
- Treuhaft, R. N., & S. T. Lowe: 1991, *AJ*, 102, 1879
- Eubanks, T. M. et al.: 1997 "Advances in Solar System Tests of Gravity." In: Proc. of The Joint APS/AAPT 1997 Meeting, 18-21 April 1997, Washington D.C. *Bull. Am. Phys. Soc.*, Abstract #K 11.05 (1997), unpublished.
- Turyshev, S. G. 1998, *BAAS*, 29, 1223
- Sovers, O. J., Fanselow, J. L., and Jacobs, C. S. 1998, 70, 1393
- Standish, E. M. Jr., Hellings, R. W. 1989, *Icarus*, 80, 326
- Yoder, C F. 1995, *Astrometric and Geodetic Properties of Earth and the Solar System*. Global Earth Physics. A Handbook of Physical Constants, AGU Reference Shelf 1.
- Standish, E. M. Jr. 1995, *Astronomical and Astrophysical Objectives of Sub-Milliarcsecond Optical Astrometry*. *IAU-SYMP*, **166**, eds. E. Hög and P. K. Seidelmann. p.109
- Standish, E. M. Jr., Newhall, X X, Williams, J. G., and Folkner, W. M. 1995, *JPL Planetary and Lunar Ephemeris, DE403/LE403*, Jet Propulsion Laboratory IOM # 314.10-127
- Folkner, W. M. *et al.* 1994, *A&A*, 287, 279

Table 16: Some astronomical parameters for the bodies in our solar system.

Object	Mean distance, AU (1900.0)	Radius $\mathcal{R}_B$ , km	Inverse mass, $\mathcal{M}_\odot/\mathcal{M}_p$	Sidereal period, yr
Sun	8.5 kpc	695,980	1.00	$2.5 \times 10^8$
Moon	384,400 km	1,738	27,069,696.00	2
Mercury	0.3870984	2,439	6,023,600.00	0.241
Venus	0.7233299	6,050	408,523.71	0.615
Earth	1.0000038	6,378.16	332,946.05	1.000
Mars	1.5237	3,394	3,098,708.00	1.881
Jupiter	5.2037	70,850	1,047.35	11.865
Saturn	9.5803	60,000	3,497.99	29.650
Uranus	19.1410	24,500	22,902.98	83.744
Neptune	30.1982	25,100	19,414.24	165.510
Pluto	39.4387	3,200	$1.35 \times 10^8$	247.687

Table 17: Some physical constants and conversion factors used in the paper.

Relativity constant:	$G/c^2 = 0.7425 \times 10^{-28}$ cm/g,
Speed of light:	$c = 2.997292 \times 10^{10}$ cm/sec,
Solar mass:	$\mathcal{M}_\odot = 1.9889 \times 10^{33}$ g,
Solar gravitational constant:	$\mu_\odot = c^{-2}G\mathcal{M}_\odot = 1.47676 \times 10^5$ cm,
Solar quadrupole coeff.:	$J_{2\odot} = (1.7 \pm 0.17) \times 10^{-7}$ ,
Solar spin moment:	$\mathcal{S}_\odot = 1.63 \times 10^{48}$ g cm <sup>2</sup> /sec,
Earth—Moon distance:	$r_{\oplus-m} = 3.844 \times 10^{10}$ cm,
Earth’s spin moment:	$\mathcal{S}_\oplus = 5.9 \times 10^{40}$ g cm <sup>2</sup> /sec,
Astronomical Unit:	AU = 1.495 978 92(1) $\times 10^{13}$ cm,
1 parsec:	pc = $3.0856 \times 10^{18}$ cm,
1 light-year:	ly = $0.94605 \times 10^{18}$ cm,
1 year:	yr = $3.155\ 692\ 6 \times 10^7$ sec,
1 day:	day = 86 400 sec,
1 sidereal day:	s_day = 86 164.091 sec,
1 microarcsecond:	$1 \mu\text{as} = 4.84814 \times 10^{-12}$ rad,
1 radian:	1 rad = $0.20627 \times 10^{12}$ $\mu\text{as}$ .